NeuroImage 191 (2019) 104–115

Contents lists available at ScienceDirect

NeuroImage

journal homepage: www.elsevier.com/locate/neuroimage

Prolonged functional development of the parahippocampal place area and occipital place area

Tobias W. Meissner [a,b,*], Marisa Nordt [a], Sarah Weigelt [b]

[a] Ruhr University Bochum, Faculty of Psychology, Universitätsstr. 150, 44801 Bochum, Germany
[b] TU Dortmund University, Faculty of Rehabilitation Sciences, Department of Vision, Visual Impairments & Blindness, Emil-Figge-Str. 50, 44227, Dortmund, Germany

ARTICLE INFO

Keywords:
Child
fMRI
High-level vision
Place
Scene perception
Development

ABSTRACT

Successful navigation of our surroundings is of high environmental relevance and involves processing of the visual scenery. Scene-processing undergoes a major behavioral improvement during childhood. However, possible neural changes that underlie this cognitive development in scene perception are understudied in comparison to other stimulus categories. We used a functional magnetic resonance imaging (fMRI) scene localizer and behavioral recognition and memory tasks in 7-8-year-olds, 11-12-year-olds, and adults to test whether scene-selective areas—the parahippocampal place area (PPA), the retrosplenial cortex (RSC), and the occipital place area (OPA)—show a change in volume and selectivity with age, and whether this change is correlated with behavioral perception and memory performance. We find that children have a smaller PPA and OPA than adults, while the size of RSC does not differ. Furthermore, selectivity for scenes in the PPA and the OPA, but not in the RSC, increases with age. This increase seems to be driven by both increasing responses to preferred stimuli and decreasing responses to non-preferred stimuli. Our findings extend previous knowledge about visual cortex development by unveiling the underlying mechanisms of age-related volume and selectivity increases in the scene network especially elucidating the poorly understood development of the OPA.

1. Introduction

Having a sense of *place* becomes environmentally relevant for humans when their self-guided explorations' range of motion drastically increases—typically in middle childhood. fMRI studies in adults have identified a network of three high-level visual cortical areas, which reliably show higher activation for scenes over other stimulus categories, e.g. objects. This functionally defined scene network comprises the parahippocampal place area (PPA, Epstein and Kanwisher, 1998), the retrosplenial cortex (RSC, O'Craven and Kanwisher, 2000), and the occipital place area (OPA; also called transverse occipital sulcus, TOS; Dilks et al., 2013; Ganaden et al., 2013; Grill-Spector, 2003; Hasson et al., 2003). In adults, each area's response properties and contribution to scene processing have been extensively elucidated (e.g. Bettencourt and Xu, 2013; Dilks et al., 2011; Epstein et al., 2007; Epstein et al., 2005).

Despite this plethora of research in adults, developmental studies on the scene network are scarce. Often, findings come up as a by-product of face perception research that focuses on the ventral temporal cortex and frequently uses scenes—and the PPA—as a control condition. Accordingly, only few studies have hitherto shed light on the development of the PPA in children, only one study has targeted the RSC in children (Jiang et al., 2014), and to the best of our knowledge no study has yet investigated the OPA in children. In detail, conflicting findings are reported for PPA maturation: An age-related increase (between age 7 and adulthood) of PPA volume was found for the left hemisphere (Golarai et al., 2007), or not at all (Scherf et al., 2007, 2011), whereas an age-related increase of the PPA's response magnitude to scenes was found in the right hemisphere (Chai et al., 2010), or not at all (Jiang et al., 2014). Concerning the RSC, the one developmental study including this region does not suggest age-related differences in RSC volume or scene-selectivity in a localizer task (Jiang et al., 2014).

Characterizing the scene network's neural development is important as it might contribute to the marked behavioral visual scene processing development observed in late childhood. In comparison to younger children, older children perform better at scanning the given task-appropriate and most informative parts of a scene (e.g. Vurpillot, 1968), have a larger field of view for processing scenes (e.g. Mackworth and Bruner, 1970), are less easily distracted by irrelevant information in

* Corresponding author. TU Dortmund University, Faculty of Rehabilitation Sciences, Department of Vision, Visual Impairments & Blindness, Emil-Figge-Str. 50, 44227, Dortmund, Germany.
E-mail addresses: tobias.meissner@rub.de (T.W. Meissner), marisa.nordt@rub.de (M. Nordt), sarah.weigelt@tu-dortmund.de (S. Weigelt).

https://doi.org/10.1016/j.neuroimage.2019.02.025
Received 10 October 2018; Received in revised form 15 January 2019; Accepted 9 February 2019
Available online 11 February 2019

a scene (e.g. Munsinger and Gummerman, 1967), and need less information for their inference about the contents of a scene (Day, 1975). Alongside perception, memory for scenes also improves with age from 6 years to 11 years and even further until adulthood (Dirks and Neisser, 1977; Mandler and Robinson, 1978). In summary, children younger than 10 years show lower behavioral performance in scene processing, while most 12-year-olds perform as well as adults. One underlying factor for this notable behavioral development might be the maturation of the visual cortical scene processing network.

Here, using an fMRI scene localizer, we chart the functional development of the known scene network in middle childhood (7–8 years), late childhood (11–12 years), and adulthood (20–24 years). The objectives of our study are three-fold: First, we aim to examine the development of scene network regions PPA, RSC, and OPA in terms of their detectability, spatial topography, and volume. Second, we aim to investigate the development of scene network regions in terms of their scene-selectivity, as well as the underlying mechanism and precise spots of selectivity changes. Third, using behavioral perception and memory tasks, we aim to explore whether neural development is associated with behavioral changes in the scene processing domain.

2. Methods

2.1. Participants

Data of 13 children aged 7–8 ($M = 7.46$, $SD = 0.52$, 6 females; henceforth: 7-8yo), 13 children aged 11–12 ($M = 11.23$, $SD = 0.44$, 9 females; henceforth: 11-12yo) and 13 adults aged 20–24 ($M = 20.69$, $SD = 1.25$, 6 females) were analyzed for this study. All participants were healthy, had normal or corrected-to-normal vision, and had been born at term. No participant had past or current neurological or psychiatric conditions, or structural brain abnormalities. The original sample contained three additional 7-8yo and two additional adults that were excluded in a matching procedure for explained variance by the GLM (see 2.3.3). Children were recruited through flyers and booths at schools, sport clubs, youth leisure centers, and by direct contact with parents of former participants. Adults were recruited through flyers at the Ruhr University Bochum and via social media. Adults received course credit or 30 EUR for their participation; children received small toys and a 15 EUR voucher for a book or toy store.

2.2. Neuroimaging

Magnetic resonance images were acquired at the Ruhr University Bochum teaching hospital Bergmannsheil on a 3.0T Archieva scanner (Philips, Amsterdam, The Netherlands) using a 32-channel head coil. Participants were instructed to lie still and relax. Padding was supplied to minimize head movements. To reassure children and parents as well as to provide the possibility for low-threshold contact, children were accompanied by one of the experimenters in the scanner room throughout the entire procedure. Children who had not participated in an MRI study before were accustomed to the scanning environment, experimental procedure, and tasks in a custom-built mock scanner at least one day prior to scanning. Children with MRI experience in our scanner were familiarized with the experimental procedure and tasks on the day of scanning.

First, we obtained a T1-weighted high-resolution anatomical scan of the whole head (MP-RAGE, TR = 8.10 s, TE = 3.72 ms, flip angle = 8°, 220 slices, FOV = 240 mm × 240 mm, matrix size = 240 × 240, voxel size = 1 mm × 1 mm × 1 mm). We then obtained functional images in a scene localizer block design experiment using a blood oxygen level dependent (BOLD) sensitive T2-weighted sequence across 33 slices (TR = 2000 ms, TE = 30 ms, flip angle = 90°, FOV = 240 mm × 240 mm, matrix size = 80 × 80, voxel size = 3 mm × 3 mm × 3 mm, slice gap = 0.4 mm).

2.2.1. Visual stimuli features and presentation

During fMRI localizer scans, participants viewed color photograph images of scenes and objects, as well as gray rectangles in the rest condition (Fig. 1). Scenes and objects were downloaded from the internet or from image databases including the SUN database (Xiao et al., 2010, 2016), the Pasadena Houses 2000 database (Helle and Perona, 2000), and the BOSS database (Brodeur et al., 2010, 2014). Scene stimuli included natural and man-made outdoor scenes as well as private and public indoor scenes. All scenes showed the ground/floor and the sky/-ceiling and did not contain humans or animals. Objects' size ranged from hand-sized objects to larger-than-body objects. Objects were presented on a background that consisted of randomly assigned scrambled (1-pixel-level) versions of the scene stimuli to ensure a comparable average background luminance and colorfulness for the scene and object categories. Fourteen gray rectangles in different shades (RGB 45/45/45 to RGB 240/240/240 in steps of 15) were used for the rest condition to facilitate a 1-back task not only during scene and object, but also during rest blocks, ensuring that participants attended to the stimulus display throughout the entire run.

Stimuli were presented at a size of 440 × 330 pixel (~16° × 13° visual angle) on a gray background (RGB 112/112/112) via a VisuaStim Digital goggle system (FOV: 30° × 24°, 800 × 600 pixel, Resonance Technology Inc., CA, USA). The experiment was run with MATLAB (version 2012a, RRID: SCR_001622) and Psychtoolbox extensions (version 3.0.9, RRID: SCR_002881, Brainard, 1997; Kleiner et al., 2007; Pelli, 1997) on a Dell Latitude E5540 machine (4 GB RAM, Intel Core i5-4300U CPU, Dell Technologies Inc., Round Rock, TX, USA) and Windows 7 Professional 32-bit as operating system (Microsoft Corporation, Redmond, WA, USA).

2.2.2. Localizer design

Participants viewed a total of four 182 s long runs, each comprising 13 blocks (Fig. 1). There were two possible palindromic sequences for scenes (S), objects (O), and rest blocks with gray rectangles (R). Run sequence type A was RSORSOROSROSR. In run sequence type B, the order of scene and object blocks was reversed: ROSROSRSORSOR. Participants performed two type A and two type B runs in a pseudo-random order (S1 Text). One block contained 14 image presentations at 1 Hz for 970 ms followed by a 30 ms background screen. Scene and object stimuli were not repeated, except for one random occasion per block (1-back task). To reduce possible visual fatigue during stimulus presentation, six images appeared at the center of the screen within each 14-image block while eight images appeared with an offset of 4 pixels to the right/left/top/bottom or a combination of those.

2.2.3. Data preprocessing

Preprocessing of fMRI data was performed using BrainVoyager (Version 20.2 for 64bit Windows, RRID: SCR_013057) and included slice scan time correction, 3D motion correction, and temporal filtering. For

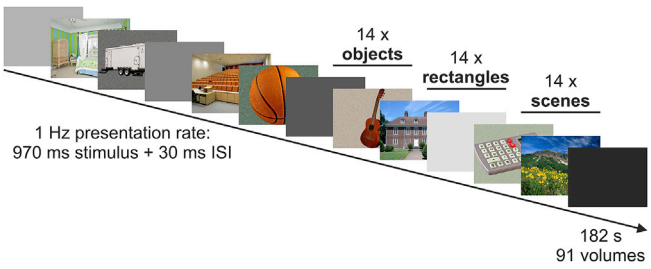

Fig. 1. fMRI localizer stimuli design for an A-type run. For each block, one exemplary stimulus is shown. In the actual experiment, each scene or object was only presented once, except for 1-back task events. In the rest blocks, however, all 14 gray rectangles were repeated at a random order in each block (also including a 1-back-task). For better visibility, stimuli are depicted without the gray surrounding background of the original experiment.

the slice scan time correction procedure, we used cubic spline interpolation. For the 3D motion correction, we used a trilinear/sinc interpolation on the whole data set with a maximum of 100 iterations to fit a volume to the reference volume. As the localizer was split into several runs, we also performed an intra-session alignment with the volume following the anatomical scan as a reference. For temporal filtering, a high-pass filter (GLM-Fourier, 2 sines/cosines) was applied. Preprocessed functional data of the first runs was co-registered with the anatomical scans. Previous studies have confirmed the feasibility of using a common stereotactic space to compare brain structure and activation of young adults and 7-8-year-old children in fMRI studies (Burgund et al., 2002; Kang et al., 2003). Thus, Talairach transformation (Talairach and Tournoux, 1988) was applied to anatomical images of all age groups semi-automatically.

2.2.4. Functional region of interest definition

For subject-specific GLM computation in BrainVoyager, separate predictors were defined for each category and each run, modeling a two-

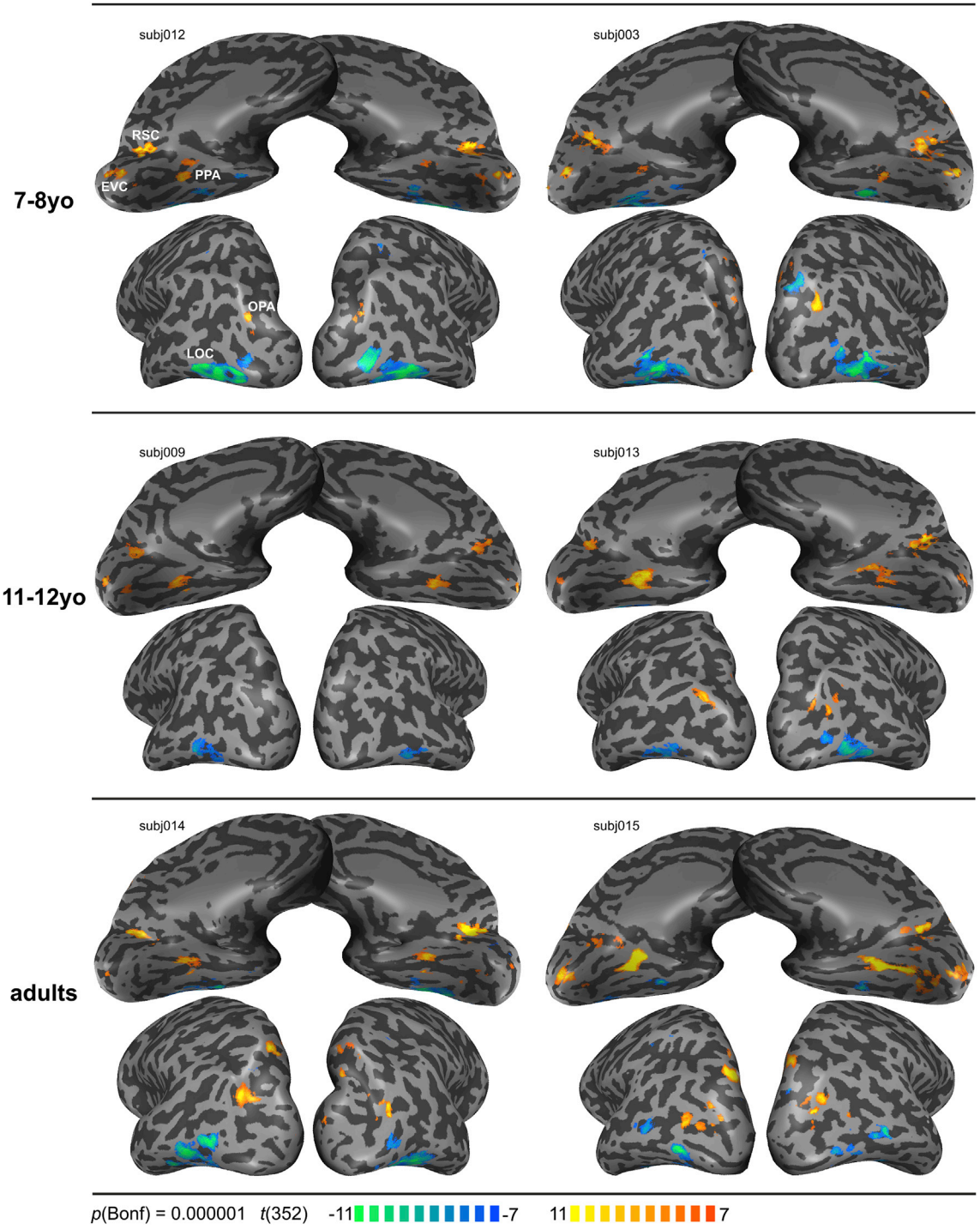

Fig. 2. Inflated cortical surfaces of two exemplary subjects per age group. Individual activation maps for the contrast scenes > objects (whole brain) based on all four runs were thresholded at p(Bonf) = 0.000001. Lower positive t-values = orange, higher positive t-values = yellow. Lower negative t-values = blue, higher negative t-values = green. Note that due to the sampling along the white-gray-matter boundary some ROIs that form a cohesive cluster in volume space (S1 Figure) can appear as smaller or as a set of smaller separate patches on the inflated surface.

Gamma hemodynamic response function. For each subject, all four localizer runs were used to define functional regions of interest (ROIs) PPA, RSC, and OPA in each hemisphere based on contiguous voxels whose contrast of scenes > objects was significant at a p(Bonferroni) = 0.000001 threshold (corresponding t-value = 7.0; S1 Figure). If there were two candidate clusters for a ROI in plausible anatomical locations, the larger one was selected. In two participants (one adult, one 11-12yo), functional clusters of PPA and RSC overlapped in one hemisphere (once left, once right). To define ROIs, these clusters were split into two at the site of the smallest connection along the z axis between PPA and RSC. The voxels in the z axis plane of the cut were not included in either ROI.

Aside from the ROIs under investigation in our study, the employed scenes > objects contrast revealed additional activation clusters (Fig. 2). In most subjects we observed relatively higher activation for scenes versus objects in early visual cortex (EVC) and relatively higher activation for objects versus scenes in the established object-selective lateral occipital complex (LOC). In some subjects we observed (mostly small) activation clusters for both scenes and objects in areas medial and superior to the OPA, on the border of superior occipital cortex and inferior parietal cortex (Fig. 2, subj012, subj003, subj014, subj015, cf. Nasr et al., 2011). Further, in a few subjects we observed small activation clusters at the anterior end of the calcarine sulcus and the parieto-occipital sulcus that could overlap with the area prostriata—an area that has large, equally distributed receptive fields and shows a preference for fast visual motion (Fig. 2, subj015, left hemisphere, Mikellidou et al., 2017). Although not investigated or discussed any further here, we suggest that given its characteristics, area prostriata could potentially play a part—similar to the scene network—in visually guided navigation.

As indicated by the scarce amount of literature on the OPA compared to the PPA and RSC, the OPA might be more elusive in children than other scene-selective areas (no investigation in the relevant developmental studies, Golarai et al., 2007; Jiang et al., 2014; Pelphrey et al., 2009; Scherf et al., 2011; Scherf et al., 2007, despite early discovery; Grill-Spector, 2003; Hasson et al., 2003). Moreover, we employed a rather conservative threshold to prevent the PPA and RSC clusters from extending and overlapping. Consequently, using the same statistical threshold to detect all scene-selective areas resulted in significantly lower OPA detection rates and less informative subsequent analyses within the OPA in our study (see 3.1). To achieve a more accurate characterization of the OPA's development, we conducted a reanalysis of our data with a more liberal detection threshold of p(uncorrected) = 0.00001 (corresponding t-value = 4.5) for the OPA, dubbed OPA-lib. However, as expected, while the more liberal threshold led to a higher detection rate in children, it resulted in a large expanse of original OPA activity into surrounding activations in six adults. In these subjects, four rOPA-lib and three lOPA-lib clusters included occipital cortex or RSC activation or spanned both hemispheres and therefore could not be defined as OPA-lib clusters and were not included in the analysis. Note that the exclusion of large OPA-lib clusters in adults due to unfeasible delineation reduces the chance of detecting age-related increases in OPA cluster size.

To analyze brain responses *within ROIs*, we split our localizer data in half, using odd runs to functionally define the scene-selective ROIs like described above, but with a p(Bonferroni) = 0.001 threshold (corresponding t-value = 6.0). For the OPA-lib reanalysis we used a more liberal detection threshold of p(uncorrected) = 0.0001 (corresponding t-value = 4.0). Each subject's activity in even runs was then analyzed within their individually defined ROIs based on odd run activity (Kanwisher et al., 1997). We decided to use the first and third run—i.e. odd runs—to define ROIs to analyze brain responses within ROIs (see 2.2.4) to ensure having at least one run for ROI detection and one run for selectivity analysis in the case of a child terminating the experiment early. For details on the distribution of sequence-types A and B (S1 Text) in odd runs, please refer to S2 Text. In one 11-12yo subject functional clusters of lPPA and lRSC overlapped but could be split manually. In two adults the rOPA-lib was not definable due to its overlap with other activity clusters and was therefore dropped from the analysis.

2.2.5. Shell and core region of interest definition

To determine which mechanisms contribute to the age-related volume increase in ROIs, we compared the functional profile of children's voxels that will most likely become part of children's ROI during maturation with the functional profile of adult's voxels that were most likely not yet part of adult's ROI when they were still children (cf. Golarai et al., 2007). Accordingly, we created shell ROIs for children and adults as follows (see 3.5): Children's odd-run-defined ROIs were individually dilated in a shape-preserving manner until the mean children's dilated ROI size was equal to the mean adult's ROI size. Next, we excluded children's original ROI voxels from the dilated-to-adult-sized ROIs, leaving shell ROIs of voxels that are adjacent to the children's original ROIs and extend to the assumed future mature ROI boundary. Adult's odd-run-defined ROIs were individually shrunk in a shape-preserving manner until the mean adult's shrunk ROI size was equal to the mean children's ROI size. A minimum size of one (centroid) voxel was kept for the rPPA of one adult in which all voxels were excluded during shrinking. Next, we excluded adult's shrunk-to-child-sized ROIs from adult's original ROIs, leaving shell ROIs of voxels that are part of adult's original ROI periphery but exclude an inner core region.

Furthermore, to determine if the functional development is restricted to areas into which a ROI expands during maturation, we compared the functional profile of children's ROIs with adult's core ROI regions, i.e., voxels that were most likely already part of adult's ROI when they were still children (see 3.5). Here, we used the shrunken adult ROIs from the first shell ROI creation step as adult's core ROIs.

2.3. Neuroimaging data quality control

Before running statistical analyses, we ensured similar levels of fMRI data quantity and quality for children and adults by comparing and, if necessary, controlling several measures outlined below that could influence detection power or confound the BOLD signal quality between age groups (Thomason et al., 2005), despite reports that question an influence of moderate differences in BOLD signal quality (Golarai et al., 2007). Further details for each of the following quality control measures are given in S3 Text and S2 Figure.

2.3.1. Anatomical volume

To control for the possibility that increases in functional cluster volume were not primarily age-related but driven by an increase in the underlying anatomical structure volume, we identified anatomical regions that correspond to the functional scene network ROIs and compared their gray matter volume between age groups (S3 Text, S2 Figure a). Separate univariate ANOVAs for each anatomical region with between-subject factor age group revealed that none of the anatomical regions showed an age-related increase in gray matter volume from childhood to adulthood. Therefore, it is unlikely that possible increases in functional ROI volumes can be explained by volume increases of the underlying anatomical structures.

2.3.2. Motion

We controlled for different magnitudes of subject motion between age groups during functional scans by excluding three runs from two 7-8yo that contained volume-to-volume motion $\geq$3 mm (x, y, z) or $\geq 3°$ (pitch, roll, yaw) prior to any analyses. However, due to having less data, these subjects' detection power was diminished. Consequently, with the same statistical threshold (see 2.2.4), the probability of detecting a ROI became smaller, biasing the detection rate results. Even if a ROI was detected, the ROI would most likely have been smaller, biasing the ROI volume results. To counter this confirmatory bias regarding our hypothesis of an age-related increase of ROI volume, three runs from two adults as well as from two 11-12yo were selected at random and discarded, thereby evening out the number of runs in each age group.

ANOVAs on mean volume-to-volume motion, maximal total motion, and mean between-run motion indicated that all age groups moved to a similar extent in the scanner, rendering possible age group differences in brain activation due to subject motion unlikely (S3 Text, S2 Figure b).

2.3.3. GLM fit

We analyzed the percentage of time course variance that can be explained by the GLM as a goodness of fit measure of the GLM before running any localizer-specific analyses (S3 Text, S2 Figure c). As a one-way ANOVA across all ROIs indicated that 7-8yo, 11-12yo, and adults differed in the percentage of explained GLM variance, we excluded three 7-8yo children with the lowest and two adults with the highest explained variance. A re-run of the ANOVA did not detect significant age group differences anymore. To further compare age groups' BOLD signal properties independently of the perceived stimuli, we quantified the percentage of BOLD signal fluctuations in each ROI and each subject across all runs. A one-way ANOVA across all ROIs indicated that age groups did not differ in their BOLD signal fluctuation during rest blocks. Thus, possible age group differences cannot be attributed to a better GLM fit or a higher BOLD signal fluctuation during rest blocks in specific age groups. All analyses reported in this were run without these five subjects.

2.3.4. Attention towards stimuli (1-back task)

To ensure that participants attended to the stimuli during the fMRI scans, participants performed a 1-back task, in which they had to press a button if two consecutive stimuli were identical. Accuracy during scene and object presentation was consistently high for all age groups, indicating that participants of all age groups were highly attentive to the stimuli. To control for possible differences in attention between stimulus categories, we conducted a 3×2 mixed ANOVA with between-subject predictor age group (7-8yo, 11-12yo, adults), within-subject predictor stimulus category (scenes, objects) and accuracy as the dependent variable (S3 Text, S2 Figure d). The mixed ANOVA revealed that accuracy increased with age but did not differ between stimulus categories. Most importantly, the amount of attention given to the two stimulus categories increased with age to the same extent.

2.4. Behavioral memory and perception tasks

To explore a possible brain-behavior relationship, participants completed a memory task and a perceptual discrimination task for the two stimulus categories scenes and objects on the day of the mock scanner training (S3 Figure). The order of tested stimulus categories was randomized. To control for possible differences of developmental trajectories in the two tasks due to the use of different stimuli, participants saw the same stimuli in the memory and the perceptual discrimination task. To ensure that memory performance was not affected by prior encounter with the stimuli, the memory task was always tested before the perceptual discrimination task. Participants completed a short training for the memory and perceptual discrimination task with a different category (animal faces).

2.4.1. Experimental setup

The behavioral experiment was conducted on a 12.5"-screen multi-touch display touch tablet device (ASUS T300F, Taipeh, Taiwan; 27.6 cm × 15.5 cm screen, ~38° × 22° visual angle, resolution 1366 × 768 pixel, Windows 8.1 64-bit operating system) in landscape orientation and full screen mode. Responses were recorded via touchscreen, while participants sat in front of the tablet with an approximate viewing distance of 40 cm.

2.4.2. Stimuli

The stimuli consisted of houses and cars (representative for scenes and objects) as used in a prior experiment (Weigelt et al., 2014; S3 Figure c). For the memory task, we used ten target-distractor pairs for houses and ten target-distractor pairs for cars, i.e. 40 stimuli in total. For the perceptual discrimination tasks, we used the original target-distractor pairs to create morphs in steps of 5%. This morphing procedure resulted in 380 new images (20 target-distractor pairs in 19 steps ranging from 5% to 95%). All stimuli were grayscale and 430 × 280 pixel (~11° × 7° visual angle).

2.4.3. Memory task

The memory task consisted of an encoding phase and a recognition phase (S3 Figure a). In the encoding phase, participants viewed and sorted ten target stimuli according to the number of rooms in the house (two rooms vs any other number of rooms) or the type of car (hardtop vs convertible) in a two-alternative forced choice task. The target stimuli were presented centrally in a field on the screen once the participant tapped onto the field. Sorting boxes with sketches corresponding the two alternatives flanked the central target stimulus to the left and right. To ensure proper encoding, participants viewed the target stimuli for a 3-s delay and engaged with the target stimuli by dragging and dropping the target onto one of the sorting boxes. There was no time restriction for encoding and sorting. The inter-trial-interval was 1 s. In the recognition phase, participants successively viewed ten stimulus pairs consisting of the familiar target and a new distractor stimulus of the same category and same type of car or house presented on each side of the display (S3 Figure a). They were asked to decide which stimuli they recognized from the learning phase by dragging and dropping a centrally presented candy to one of the stimuli. There was no time restriction for the recognition phase, as we focused on the accuracy of responses. We calculated a recognition memory score for each stimulus category which ranged between zero and one and indicated the ratio of correctly recognized stimuli to all (ten) presented stimuli of the encoding phase.

2.4.4. Perceptual discrimination task

This task measured perceptual discrimination threshold for scenes and objects, i.e. the mean difference between morph image pairs necessary to discriminate them. Each trial consisted of a sample display, in which a sample stimulus was presented centrally for 1.5 s and a test display, following immediately, which showed the sample stimulus and morph distractor stimulus side by side (S3 Figure b). Participants were asked to drag a centrally presented candy to the sample stimulus as a two-alternative forced choice match-to-sample task. The sample stimuli were 5% and 95% morph images between the target-distractor pairs from the memory task. Thus, each memory task target-distractor pair yielded two sample images. For each sample stimulus, morph distractors were created in 5% morph steps: 10%–95% for the 5%-sample stimulus and 90%–5% for the 95%-sample stimulus (S3 Figure b).

Two parallel staircases worked in a one-up-three-down procedure in steps of 5% to select which percentage of morphing the distractor would have. One staircase moved upwards, i.e. always using the 95%-sample stimulus and starting with the 5%-morph as the first distractor. The other staircase moved downwards, i.e. always using the 5%-sample and starting with the 95%-morph as the first distractor. For each correct answer, the morph-distractor's similarity towards the sample increased by one step, i.e. 5%, while an error decreased its similarity by three steps, i.e. 15%. Each staircase ran until a total of eight reversals were detected, with morph pairs being presented in a randomized order. A reversal was counted when the participant made an error or when the participant tried to surpass the minimum of 5% morph distance between target and morph-distractor. In the latter case, the morph-distractor values did not change. The first 25% of each staircase were a safe zone, in which errors did not count as a reversal until the first error outside of this safe zone was committed. We defined the perceptual discrimination threshold as the mean morph distance between sample and morph-distractor across all 16 reversals.

2.5. Experimental design and statistical analysis

Statistical analysis of behavioral and neuroimaging data was

performed using R (version 3.2.2, RRID: SCR_001905, R Core Team, 2015) in RStudio (version 0.99.491; RRID: SCR_000432). As we employed a variety of different statistical tests, details for each test are described in the corresponding methods and results sections for better comprehensibility.

3. Results

In the present study we used an fMRI scene localizer to determine the decectibility, volume, location, and degree of scene-selectivity of the PPA, RSC, and OPA in three age groups. We tested for effects of age across thirteen 7-8yo, 11-12yo, and adults (20-24yo) to chart the development of the scene-network from middle childhood to adulthood. Further, to understand whether changes in volume or scene-selectivity are associated with behavior, we made use of additional behavioral perception and memory tasks to explore brain-behavior relationships in our data.

3.1. Detection rate

We examined whether our functional localizer detected ROIs in all age groups with a similar probability using Fisher's exact test. For the left and right OPA, as well as for the rPPA, we found an association between age group and detection frequency of ROIs that was driven by a higher detection rate in adults compared to 7-8yo and 11-12yo children (lOPA: 7-8yo: 46.15%, 11-12yo: 46.15%, adults: 100.00%, $\chi^2(2) = 10.92$, $p = .004$; rOPA: 7-8yo: 53.85%, 11-12yo: 69.23%, adults: 100.00%, $\chi^2(2) = 7.53$, $p = .023$, rPPA: 7-8yo: 76.92%, 11-12yo: 100.00%, adults: 100.00%, $\chi^2(2) = 6.5$, $p = .039$, Fig. 3a, numbers of detected ROIs in top row). The detection rate for the RSC did not differ in both hemispheres.

Despite the significantly lower detection rate in the rPPA, we judged the number of observations as high enough for further analyses. In contrast, due to the considerable differences in detection rates for the OPA in both hemispheres, we conducted a reanalysis with a more liberal detection threshold for the OPA, thus called OPA-lib, to achieve comparable detection rates for all age groups. After the reanalysis, lOPA-lib and rOPA-lib were detected equally often in each age group (lOPA-lib: 7-8yo: 84.61%, 11-12yo: 100.00%, adults: 81.82%, $\chi^2(2) = 2.45$, $p = .290$; rOPA-lib: 7-8yo: 92.31%, 11-12yo: 92.31%, adults: 81.81%, $\chi^2(2) = 0.88$, $p = .643$, Fig. 3b, numbers of detected ROIs in top row).

To sum up, using standard statistical thresholds that prove sensible for delineating scene-selective ROIs in adults result in an underestimation of OPA presence in children. As we are the first to map the OPA in children, comparable data on detection rates are not available. However, our detection rates for both PPA and RSC in children are in line with previous findings (cf. Golarai et al., 2007; Jiang et al., 2014).

3.2. Volume

We investigated whether there were age-related changes in the volume of PPA, RSC, and OPA using univariate ANOVAs with between-subject factor age group for each functional ROI. In our main analysis, we assumed that non-detected ROIs would still emerge later in life and thus included them in the analysis with a ROI size of 0 mm^3. We found significant age-related volume increases for the PPA, OPA, and OPA-lib in both hemispheres, but not for the left or right RSC (Fig. 3a, b, S1 Table). Planned comparisons using t-tests indicated that these age group differences were driven by larger ROIs in adults compared to children, while 7-8yo and 11-12yo children did not differ in their ROI volume (S2 Table). We replicated this pattern of results in a supplementary analysis that assumed non-existence of non-detected ROIs with the exception of the lOPA, which did not exhibit an age-related volume increase (S4 Figure, S1 Table). Note that none of the anatomical structures underlying the functional ROIs PPA, RSC, and OPA showed a volumetric increase with age (see 2.3.1). Thus, it is unlikely that our results are driven by changes in these underlying anatomical structures.

A separate set of ROIs was defined based on data from odd runs only (see 2.2.4). These ROIs were used to analyze scene-selectivity data from even runs to avoid circular analyses (see 3.4). A re-run of the volume ANOVA with the odd-run-defined ROIs revealed the same pattern of results as the ANOVA for the ROIs based on all four runs for the PPA and the RSC as well as a very similar pattern of results for the OPA and OPA-lib (S5 Figure, S5 Text).

In summary, our data speak in favor of a prolonged volumetric increase of both PPA and OPA, but not RSC, notably beyond 12 years of age and hence extending the behavioral scene perception development documented in the literature so far.

3.3. Spatial topography

To assess whether spatial topography of the functional scene network ROIs differed between age groups, we calculated MANOVAs with x-, y-, and z Talairach centroid coordinates as dependent variables and age group as between-subject predictor for each ROI (Table 1). Each individual ROI centroid was defined by calculating the mean value for each axis (x, y, z) across all the ROI's voxels. Using Pillai's trace, we found all ROIs, except for the lPPA, to be located at similar positions in all age groups (lPPA MANOVA: $V = 0.47$, $F(2,32) = 3.15$, $p = .009$; post-hoc univariate lPPA ANOVAs: x: $F(2,32) = 4.30$, $p = .022$, $\eta^2 = 0.212$; y: $F(2,32) = 0.33$, $p = .717$, $\eta^2 = 0.021$, z: $F(2,32) = 6.21$, $p = .005$, $\eta^2 = 0.280$). With increasing age, the lPPA seemed to be located more medial and more inferior. However, the absolute maximal difference in

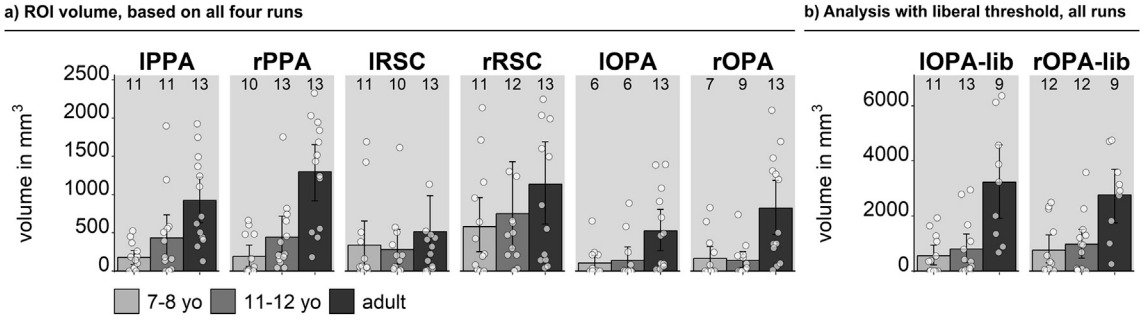

Fig. 3. ROI volume and detection rate based on all four runs. Light gray = 7-8-year-old children (n = 13), medium gray = 11-12-year-old children (n = 13), dark gray = adults (n = 13). Error bars show 95% confidence intervals of the mean. Numbers at the top indicate in how many subjects a given ROI was detected. The size of non-detected ROIs was set to 0 mm^3. (a) ROI definition based on a ROI detection threshold of p(Bonferroni) = 0.000001. To achieve a better display, individual data points above 2500 mm^3 are not displayed (missing: adult lRSC 2935 mm^3; adult rRSC 3381 mm^3; 11-12yo rRSC 4210 mm^3). For a descriptive explanation of the high variability of RSC volume, please refer to S4 Text. (b) OPA definition with a more liberal ROI detection threshold of p(uncorrected) = 0.00001. Note that the scale of (b) differs from (a).

mean lPPA locations between age groups was very small (3 mm). We inspected every function-to-structure registration—applying manual correction if necessary—and are therefore confident that this result is not due to a methodological artifact that affected children or adults in particular. This finding contrasts reports by Scherf et al. (2011), who found stable lPPA locations but a slightly (3–4 mm) more medial rPPA location in children. Yet, all other studies that reported ROI locations across age groups found stable PPA representations across age in both hemispheres (Golarai et al., 2010, 2017; Pelphrey et al., 2009; Scherf et al., 2007), and the absolute differences in our and Scherf et al.'s study—especially in relation to the large size of the PPA—were rather small. Thus, the scene-network's topography might be considered rather stable from middle childhood to adulthood. Regarding adult ROI locations, our reported coordinates are reconcilable with the literature (for an overview see Nasr et al., 2011).

Although ROI locations did not differ between age groups, they might still be more variable in younger age groups compared to adults (for an analysis of adults see Zhen et al., 2017). Therefore, we examined if the variability of ROI coordinates differed between age groups by conducting MANOVAs with the *absolute residuals* of x-, y-, and z Talairach centroid coordinates as dependent variables and age group as between-subject predictor for each ROI. Still, using Pillai's trace, we found differences in the topographical variability between age groups in the lPPA and the rPPA only (lPPA MANOVA: $V = 0.36$, $F(2,32) = 2.28$, $p = .048$; post-hoc univariate lPPA ANOVAs: x: $F(2,32) = 5.62$, $p = .008$, $\eta^2 = 0.260$; y: $F(2,32) = 1.45$, $p = .25$, $\eta^2 = 0.083$, z: $F(2,32) = 0.88$, $p = .427$, $\eta^2 = 0.052$; rPPA MANOVA: $V = 0.50$, $F(2,33) = 3.52$, $p = .005$; post-hoc univariate rPPA ANOVAs: x: $F(2,33) = 1.82$, $p = .178$, $\eta^2 = 0.099$; y: $F(2,33) = 7.02$, $p = .003$, $\eta^2 = 0.298$, z: $F(2,33) = 4.37$, $p = .021$, $\eta^2 = 0.209$). In the lPPA, topographical variability along the x-axis decreased with age. In the rPPA, topographical variability along both y- and z-axis increased from 7-8yo to 11-12yo, only to decrease again until adulthood (Table 1). However, in general, ROI coordinate variability was low, i.e. 81.5% or 79.6% of all coordinate SDs (including OPA or OPA-lib) were $\leq$5 mm.

In summary, scene-selective ROIs seem to be topographically stable across age from middle childhood to adulthood, despite possible small changes in PPA location. Moreover, interindividual centroid coordinate variability is low.

Table 1
Talairach coordinates of ROI mean center of gravity based on all four localizer runs.

ROI	age group	x (SD)	y (SD)	z (SD)
lPPA	7-8yo	−26 (3)	−44 (4)	−4 (2)
	11-12yo	−24 (3)	−45 (5)	−5 (2)
	adults	−23 (1)	−44 (3)	−7 (2)
rPPA	7-8yo	23 (4)	−42 (2)	−5 (2)
	11-12yo	22 (4)	−42 (6)	−7 (4)
	adults	24 (2)	−42 (3)	−8 (2)
lRSC	7-8yo	−18 (4)	−57 (4)	12 (4)
	11-12yo	−16 (5)	−58 (3)	14 (4)
	adults	−17 (3)	−56 (5)	12 (4)
rRSC	7-8yo	20 (4)	−55 (2)	15 (2)
	11-12yo	17 (4)	−55 (3)	15 (5)
	adults	17 (3)	−55 (3)	15 (3)
lOPA	7-8yo	−30 (10)	−76 (7)	23 (12)
	11-12yo	−34 (5)	−80 (3)	23 (6)
	adults	−29 (5)	−78 (3)	21 (8)
rOPA	7-8yo	30 (4)	−76 (3)	24 (10)
	11-12yo	32 (7)	−76 (5)	25 (8)
	adults	32 (4)	−76 (5)	20 (6)
lOPA-lib	7-8yo	−30 (8)	−78 (6)	22 (9)
	11-12yo	−32 (4)	−77 (5)	23 (9)
	adults	−29 (5)	−78 (2)	21 (8)
rOPA-lib	7-8yo	33 (6)	−75 (3)	23 (8)
	11-12yo	32 (7)	−75 (5)	26 (8)
	adults	32 (4)	−74 (4)	20 (6)

3.4. Scene-selectivity

To address the question whether scene-selectivity within ROIs changes with age, we split our localizer data in half, using odd runs to define our ROIs and even runs to assess scene-selectivity (see 2.2.4). We calculated a scene-selectivity index d' (Green and Swets, 1988) like in previous studies (e.g. Afraz et al., 2006; Grill-Spector et al., 2007) as $d' = \frac{\mu_{scenes} - \mu_{objects}}{\sqrt{\frac{1}{2}(\sigma^2_{scenes} + \sigma^2_{objects})}}$ where μ is the mean and σ is the standard deviation.

ANOVAs for each ROI with between-subject factor age group and scene-selectivity as the dependent variable revealed significant age-related increases of scene-selectivity in both hemispheres of OPA and OPA-lib, as well as in the lPPA (and a non-significant trend in the rPPA), but not in the RSC (Fig. 4a and b, S3 Table). Planned comparisons using t-tests revealed that age group differences were driven by higher scene-selectivity in adults compared to children, with similar scene-selectivity in 7-8yo and 11-12yo (S4 Table).

To further elucidate these age group effects, we conducted mixed ANOVAs with between-subject factor age group (7-8yo, 11-12yo, adults) and within-subject factor stimulus category (scenes, objects) for each ROI. We observed significant age group × stimulus category interactions in both hemispheres of OPA and OPA-lib only, indicating an age-related change in the scene-object brain response difference (Fig. 4c, d, S5 Table). In detail, we observed reduced responses to object representations with age in OPA and OPA-lib, while the response to scenes seems to initially dip from 7-8yo to 11-12yo, only to regain previous activation levels in adult age. However, planned comparisons used to disentangle the age group × stimulus category interactions were non-significant—possibly due to the non-linearity of the response to scenes (S6 Table).

To elucidate and interpret the underpinnings of the main effect of age for scene-selectivity in the PPA, we conducted planned comparisons on the percent signal change data. These analyses indicated that while there were no activation differences between age groups for scene stimuli, object stimuli activated children's left and right PPA to a higher degree than adults' (S6 Table).

To sum up, our results argue for an increase in scene-selectivity from middle childhood until adulthood in both PPA and OPA, but not RSC. Our analyses indicate that this age-related increase in scene-selectivity might be driven by reduced responses to objects rather than by increased responses to scenes.

3.5. Shell and core region of interest analysis

To investigate the developmental pattern of ROIs that showed an increase in volume and scene selectivity in more depth, we explored the underlying mechanisms of the volumetric expanse of PPA and OPA-lib from childhood to adulthood. To this end we defined shell ROIs in children and adults from odd runs and analyzed responses to scenes and objects from even runs. Children's shell ROIs cover the part of the cortex into which their ROI will most probably expand upon in the future. Adults' shell ROIs cover the part of the cortex that most probably marks the latest developmental expansion of their ROIs (cf. Golarai et al., 2007; see 2.2.5). For this in-depth analysis, we pooled 7-8yo and 11-12yo together in one age group as they did not differ in their ROI size (see 3.2).

PPA shells and OPA-lib shells revealed overall similar responses in children and adults (no main effect of age group) and higher response to scenes than to objects (significant main effect of category) in both hemispheres. Critically, the scene-object brain response difference increased from childhood to adulthood in all shell ROIs (significant age × category interactions; Fig. 5a, S7 Table). Post-hoc t-tests revealed that, depending on the ROI, both an age-related increase in responses to scenes as well as an age-related decrease in responses to objects contributed to the increased scene-object response difference in adults (S8 Table). These results suggest that with age, voxels immediately

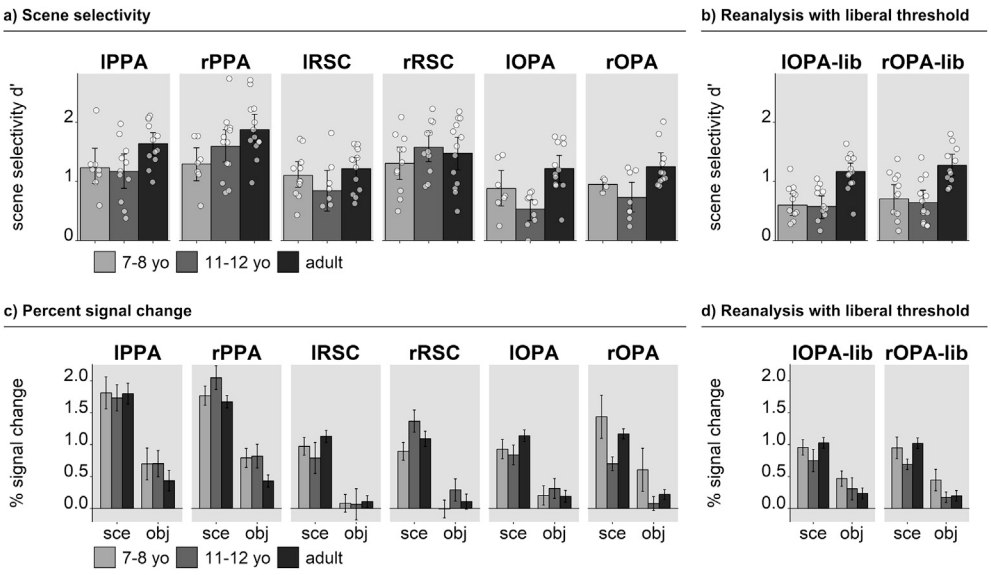

Fig. 4. Scene selectivity and percent signal change and in scene selective ROIs. ROIs were defined based on localizer runs 1 and 3 and a ROI detection threshold of p(Bonferroni) = 0.001. Scene selectivity and percent signal change were calculated based on activity from localizer runs 2 and 4. Light gray = 7-8-year-old children, medium gray = 11-12-year-old children, dark gray = adults. Error bars show 95% confidence intervals for the mean. sce = scenes, obj = objects. For a version of this figure showing the full range of individual data points, refer to S6 Figure. (a) Scene selectivity index d' in scene selective ROIs based on the % signal change data. (b) Percent signal change for each stimulus category in scene selective ROIs. Analysis of OPA scene selectivity (c) and percent signal change (d) data in larger OPAs based on a more liberal ROI detection threshold of p(uncorrected) = 0.0001.

surrounding immature scene-selective ROIs become both more responsive to preferred stimuli and less responsive to non-preferred stimuli thus driving the ROI size increase.

Further, we explored if functional development is restricted to the nascent areas of children's ROIs or if it is also evident in ROI core regions. Thus, we compared the response to scenes and objects in children's ROIs—i.e. their most probable future ROI core region—and adult's shrunken ROIs—i.e. their ROI core region and most probable ROI at childhood age—in a mixed ANOVA (scenes vs objects and children vs adults).

The core ROIs analysis revealed equal results to the shell ROI analysis for the lPPA, lOPA-lib, and rOPA-lib: Overall, responses in children and adults did not differ (no main effect of age group), responses to scenes were higher than to objects (significant main effect of category) and the scene-object brain response difference increased from childhood to adulthood (significant age × category interactions; Fig. 5b, S7 Table). In the rPPA, the same effects were evident except for a trend ($p = .060$) rather than statistical significance for the age × category interaction. Again, post-hoc t-tests revealed that both an age-related increase in scene responsiveness (except for the rPPA) as well as an age-related decrease in object responsiveness contributed to the increased scene-object response difference in adults. However, while the post-hoc tests indicated the direction of effects, only the increase of scene responsiveness in rOPA-lib and the decrease of object responsiveness in rPPA were statistically significant (S8 Table). Taken together, these results suggest that the maturation of scene selective ROIs from childhood to adulthood is not limited to increasing the scene-object response difference in areas surrounding the children's core ROI, but that the functional profile of the core ROI

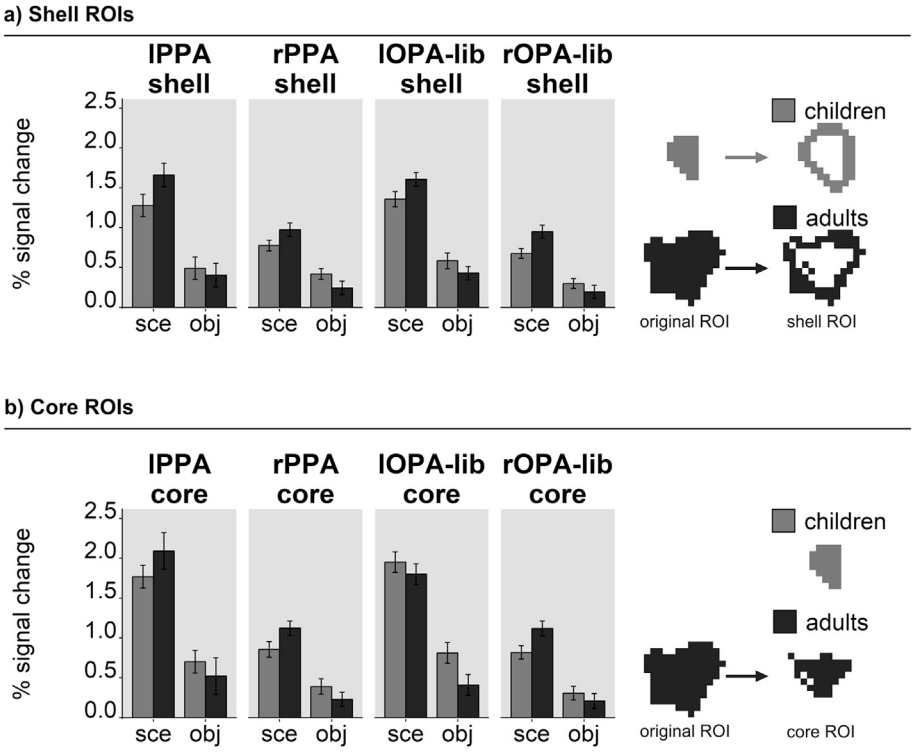

Fig. 5. Percent signal change for each stimulus category in shell (a) and core (b) regions of scene selective ROIs. Medium gray = children, dark gray = adults. Error bars show 95% confidence intervals for the mean. sce = scenes, obj = objects. For a version of this figure showing the full range of individual data points, refer to S7 Figure (a) To investigate the response to scenes and objects in brain regions that are not part of children's ROIs but will presumably become part of children's ROIs in the future, we created shell ROIs for children and adults as follows. We dilated children's ROIs until they reached adult's size. Next, we excluded each child's original ROI from the dilated ROIs, leaving shell ROIs of voxels that are adjacent to the child's original ROI. We shrank adult's ROIs individually until they reached children's size. Next, we excluded each adult's shrunk ROI from their original ROI, leaving shell ROIs of voxels that are part of adult's original ROIs but exclude an inner core region. (b) To investigate the response to scenes and objects in core regions of scene selective ROIs, we compared children's original ROIs with adult's shrunk ROIs from the first shell ROI creation.

itself is still evolving.

3.6. Brain behavior relationship

We first analyzed the behavioral memory task and behavioral perception task for effects of age, category, and age × category interactions in a mixed ANOVA. Then, we explored possible brain behavior relationships in our data, using Pearson's product-moment correlations.

Analysis of the behavioral memory task and behavioral perception task revealed that scenes were recognized and distinguished better than objects (main effect of category; memory: $F(1,36) = 17.17$, $p < .001$, $\eta^2_G = 0.133$; perception: $F(1,36) = 32.63$, $p < .001$, $\eta^2_G = 0.229$); that older participants recognized more stimuli and were better at distinguishing similar stimuli (main effect of age; memory: $F(2,36) = 5.84$, $p = .006$, $\eta^2_G = 0.181$; perception: $F(2,36) = 12.58$, $p < .001$, $\eta^2_G = .320$); and that this age-related increase in performance was similar for both stimulus types (no age × category interaction; memory: $F(2,36) = 0.05$, $p = .951$, $\eta^2_G = 0.001$; perception: $F(2,36) = 1.36$, $p = .296$, $\eta^2_G = 0.022$; S3 Figure d, e). Note that low discrimination thresholds correspond to a better perceptual discrimination.

Next, we examined whether the neural development of the cortical scene network was associated with behavioral changes in scene perception or recognition memory for scenes as measured by our tasks. To this end, we used Pearson's product-moment correlation for ROIs that showed developmental increases in volume or scene-selectivity.

First, we tested for correlations of ROI volume in both hemispheres of PPA, OPA, and OPA-lib with recognition memory for scenes, recognition memory for objects, perception threshold for scenes, and perception threshold for objects. Consequently, we lowered the significance threshold to 0.0125 (0.05/4, for four tests). No significant associations were found between ROI volume and scene or object memory (Fig. 6). At the same time, ROI volume was correlated with perception threshold for objects in the same ROIs (rPPA: $r(37) = -0.479$, $p = .0015$, lOPA-lib: $r(33) = -0.471$, $p = .0043$, rOPA-lib: $r(33) = -0.524$, $p = .0012$., S8 Figure). Likewise, we found higher ROI volume being associated with a lower scene perception threshold, i.e. a better perceptual discrimination, in the rOPA-lib ($r(33) = -0.431$, $p = .0098$) and non-significant trends in the rPPA ($r(37) = -0.385$, $p = .0155$), and the lOPA-lib ($r(33) = -0.393$, $p = .0195$, S8 Figure).

However, as ROI volume, perception thresholds, and memory were all influenced by age as shown in the previous analyses, age is likely to confound these correlations. When we calculated partial correlations of ROI volume with scene and object perception threshold and memory with age partialled out to test this assumption, we did not observe significant correlations anymore (rage of r: −0.313–0.046, all $ps > .0713$).

Second, we tested for correlations of scene-selectivity with recognition memory and perception performance. As scene-selectivity is a difference measure (see 3.4), we also calculated difference measures for recognition memory and perception threshold. Because there are no negative values for recognition memory performance or perception threshold (for details on this potential problem see Grill-Spector et al., 2007; Simmons et al., 2007) and because calculating standard deviations from the dichotomous variable memory is unreasonable, we did not, as before, use d' for scene-selectivity but $difference\ score_{task} = \frac{task_{scenes} - task_{objects}}{task_{scenes} + task_{objects}}$, where task is either recognition memory or perception threshold. However, whether or not age was partialled out, we did not observe any significant ($0.05/2 = 0.025$, for two tests) correlations of scene-selectivity in any hemisphere of PPA, OPA, or OPA-lib with the recognition memory difference score or the perception threshold difference score (range of r: −0.189–0.215, all $ps > .2921$).

All in all and unexpectedly, our data did not provide any indication for a brain-behavior relationship in terms of an association of ROI volume or scene-selectivity with our behavioral scene and object perception and memory task data.

4. Discussion

This study is the first to comprehensively chart the development of all scene network regions in middle childhood, late childhood, and adulthood. Using an fMRI scene localizer, we showed that while the PPA and RSC are readily detected in children, the OPA can only be reliably detected in children if more liberal detection thresholds are employed. We report two key findings: First, we found higher functional cluster volume and scene-selectivity in adults compared to children in both PPA and OPA, but not RSC. Second, we revealed that age-related increases in scene-selectivity in PPA and OPA were driven by higher responses to scenes and lower responses to objects with age—both in the core and the periphery of these ROIs.

4.1. Development of volume and selectivity

4.1.1. OPA

So far, no previous studies have mapped the OPA and its development from childhood to adulthood. Together with our main findings of an age-related increase in OPA volume and selectivity, the detailed developmental mechanism of an age-related increase of scene responsiveness in core and nascent OPA regions and a decrease of object responsiveness in nascent lOPA regions contributes to a more comprehensive characterization of the scene network's development from middle childhood to adulthood. Our data indicate that prolonged functional development of category-selective areas is a feature evident beyond the commonly studied boundaries of the ventral temporal cortex. Further, our results provide an incentive for future works to address the development of functional properties of the OPA.

As is known hitherto, the OPA not only engages in the recognition of scene category, but also in processing the current scene's visual features without embedding the current scene in a broader spatiotemporal context (Baldassano et al., 2016). The OPA seems to be involved in the perception of the local elements of a scene (Kamps et al., 2016) and the detailed spatial layout, extracting navigable space in a scene (Bonner and

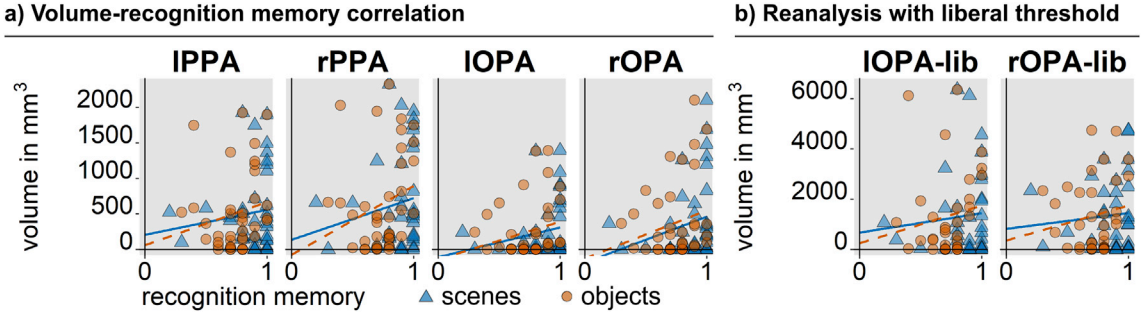

Fig. 6. Correlation of ROI volume and recognition memory for scenes and objects. Blue triangles = scenes, dark orange circles = objects. Lines = linear regression line for corresponding category. For a figure depicting the correlation of ROI volume and perception threshold, please refer to S8 Figure.

Epstein, 2017). It has however remained unclear whether the OPA represents such high-level information itself or whether it passes on low-level information crucial further along the scene processing stream (Dilks et al., 2013). Either way, the observed functional maturation of the OPA might reflect the neural adjustment or consequence to an increased need or experience in spatial orientation with increasing age.

4.1.2. PPA

Just like in the OPA, our findings of a more scene-selective and extended PPA activation in adults compared to children argue for a prolonged functional development of the scene-selective cortex. As the cytoarchitecture underlying the PPA does not seem to change from childhood to adulthood and seems unrelated to scene-selectivity (Gomez et al., 2017), two scenarios are conceivable: Either the functional changes we observe originate in structural changes that are more sublte than the structural changes that were measurable by Gomez et al. (2017). Or our data reflects purely functional changes and thus a differential development of structure and function in the PPA. This development might involve sharpening of neuronal responses tuned to scenes or objects, or a change in the firing rate of scene- or object-responsive neurons (Grill--Spector et al., 2008).

Our findings concerning functional PPA development contradict findings of some earlier studies. However, methodological differences might explain these diverging results. For instance, Pelphrey et al. (2009) defined the PPA based on separate group contrasts for children and adults, rather than based on individual activation maps. In contrast to our data, the authors report a larger PPA in children than in adults. At the same time, scene-selectivity differences between children and adults were not evident in the PPA in their data. These diverging results might stem from Pelphrey et al.'s different method of calculating category-selectivity that was previously identified as potentially problematic as it "vastly overestimates actual voxel selectivity" (Simmons et al., 2007). Two studies by Scherf et al. did not find age-related volume or scene-selectivity increases in the PPA (Scherf et al., 2007, 2011). However, both studies used movie-vignettes, rather than pictures, in their localizer. Also, to define scene-selective ROIs, the authors did not contrast scenes vs objects, but rather scene and navigation stimuli vs. object and face stimuli. Last, in one of these studies, children's neural activity was not investigated in individually defined ROIs, but in ROIs defined based on group activation of adult subjects (Scherf et al., 2007). We can only speculate about the implications of these methodological differences. Possibly, the dynamic nature of the movie-vignettes altered activation more for scenes (Cukur et al., 2016) than for faces or objects. It is also conceivable that our study elicited systematically different scanning patterns for objects and scenes due to a possibly perceived smaller extent of objects. If, on top of that, these difference interacted with participant's age, this could potentially affect response patterns in the retinotopically organized higher-level visual areas. Scherf et al.'s movie-vignettes are more dynamic and engaging stimuli, thus might have controlled for potential differences in eye-movements and therefore might explain the diverging results. Another explanation might be the different contrasts employed by our and Scherf et al.'s study. Faces elicit much lower (sometimes negative) responses in the PPA than objects (Epstein and Kanwisher, 1998). Consequently, the resulting large face-scene contrasts might have masked volume and selectivity changes that our more specific object-scene contrast was able to detect. Also, navigation stimuli might have elicited lower responses in the PPA than scenes (the specific response to navigation stimuli was not reported by Scherf et al., but see Epstein et al., 1999). Thus, to speculate, the pooling of these stimuli might have mitigated the effects that our study identified as leading to the volumetric expanse of the PPA; namely an increased scene responsiveness and a decreased object responsiveness in the nascent PPA.

More similar to our results, Golarai et al. (2007) found larger PPA volumes in adults compared to children in both hemispheres. Interestingly, the increase was not significant in the rPPA—an asymmetric pattern unexpected by the authors. Moreover, as in our study, Golarai et al. (2007) did not observe age × category interactions in the PPA.

4.1.3. RSC

Concerning the RSC, our finding of constant volume and scene-selectivity in both hemispheres across age groups agrees with the single previous study on RSC development so far (Jiang et al., 2014), suggesting that the RSC matures early, showing adult-like response properties in 7-8yo already.

4.2. Mechanisms of category-selectivity development

In an advanced analysis, we explored the origins of the increasing scene-selectivity in PPA and OPA. Our results indicate that increases in scene-selectivity seem to be driven by both increasing responses to preferred stimuli and reducing responses to non-preferred stimulus categories. This finding expands previous knowledge about the origins of category selectivity for scenes and other visual stimulus categories (Cantlon et al., 2011; Dehaene-Lambertz et al., 2018; Golarai et al., 2007).

Concerning scenes, our shell ROI analysis agrees with Golarai et al.'s study's report of an age-related increase of responses to scenes and constant responses to objects for the lPPA shell. However, for the rPPA shell, the present study, but not Golarai et al. (2007), found an age-related increase of responses to scenes and a decrease of responses to objects. Thus, results by Golarai et al. propose that lPPA maturation only entails an increase in the response to scenes in the regions surrounding children's immature lPPA, ultimately resulting in a volume increase. However, our data suggests that first, the age-related increase in responses to scenes is also evident in rPPA development; second, that this effect is accompanied by a decrease in the response to objects in the rPPA shell; and third, that functional PPA development is not restricted to the ROI shell, but also occurs in ROI core regions. Concerning other stimulus categories, evidence on how category-specificity originates or increases appears to be mixed, too. Both face-selectivity in the right fusiform face area (FFA; Golarai et al., 2007) and word-selectivity in the visual word form area (VWFA; Dehaene-Lambertz et al., 2018) appears to increase or originate by means of increasing responses to their preferred stimulus category while keeping responses to other categories largely stable. In contrast, letter-selectivity in the lateral mid-fusiform/inferior temporal gyrus seemed to increase despite stable responses to letters and with reducing responses to non-preferred categories (Cantlon et al., 2011).

Taken together, these reports suggest that there is no uniform mechanism of development for category-selectivity in higher level visual cortex. Rather, development of each category-selective area might not only be driven by distinct timelines but also by distinct underlying mechanisms.

4.3. Differential development within the scene network

Taken together, our findings suggest that while the RSC matures early, both PPA and OPA mature late. As such, these results provide further support for the notion that brain regions demonstrating a mutual category-selectivity do not necessarily possess similar developmental dynamics towards reaching adult activation expanse or magnitude (Golarai et al., 2007). What could be the reason for the differential development of the scene network? Accumulating evidence suggests a functional division of the scene processing network into two distinct parts (Baldassano et al., 2016). On the one hand, a visual network comprising the posterior PPA and the OPA processes the visual features of the current scene and has strong functional connections to early visual cortices. On the other hand, a contextual (or memory and navigation) network, comprising the anterior PPA, the RSC, and the caudal inferior parietal lobule (cIPL) establishes the connection between the current visual scene and its broader spatiotemporal context and has strong functional connections to the hippocampus. Following this two-network

theory (Baldassano et al., 2016), it seems most plausible that regions within the same sub-network follow a similar developmental pattern. This would imply that our scene localizer mapped rather posterior than anterior parts of the PPA, as PPA and OPA showed almost the same developmental pattern. Consequently, the visual sub-network would show a protracted development, while the contextual sub-network, which subserves even higher-level cognitive processes like memory and navigation, would show an early maturation. However, future studies including data from the cIPL and using a data-driven distinction between anterior and posterior PPA are needed to test these assumptions.

Another possible explanation on the differential development of high-level visual areas regards holistic processing. Golarai et al. (2007) suggested that the PPA and the FFA develop late because they represent stimuli in a holistic manner while areas that predominantly use feature-based processing like the lateral occipital complex might develop early. Consequently, our finding of a mature RSC at an early age of 7–8 years would imply that the RSC uses feature-based representations. However, much like the PPA, the functional profile and role of the RSC, e.g. viewpoint insensitivity (Park and Chun, 2009), and especially insensitivity against object presence (Harel et al., 2013). provides strong evidence for holistic representations (for an overview, see Epstein, 2008). Thus, our data is not reconcilable with the idea of holistic and feature-based representations driving the rate of development in high level visual cortex.

4.4. Brain-behavior relationship

Based on behavioral findings showing adult performance in scene processing, scene memory, and navigation around ages 11–12 (Day, 1975; Dirks and Neisser, 1977; Mackworth and Bruner, 1970; Mandler and Robinson, 1978; Munsinger and Gummerman, 1967; Vurpillot, 1968), we hypothesized an increase in scene-selective ROI volume and scene-selectivity from 7-8yo to 11-12yo, but no further development until adulthood. Yet, in contrast to our expectations, our data did not follow the developmental pattern proposed in the behavioral literature. In nearly all our analyses that showed an effect of age group (PPA and OPA), children aged 7–8 and 11–12 showed similar scores, while age effects were driven by higher scores in adults. Apparently, functional maturation of PPA and OPA seems to proceed further and beyond ages 11–12. However, at least for the PPA, there is evidence that functional maturation does not exceed ages 14–16 (Golarai et al., 2010). These assumptions are mirrored in our behavioral tablet tasks, which also show gradually increasing performance with age as well as no adult-like behavior in 11-12yo.

We expected scene-selective ROI volume and scene-selectivity to be correlated with memory and particularly perception performance for scenes. Unexpectedly, no correlations with neural parameters were found for scene memory or scene perception tasks. Partly, this finding mirrors mixed findings on an association between scene-recognition memory and lPPA volume (Golarai et al., 2007, 2010). Possibly, our findings indicate that changes in other brain regions such as the hippocampus, the visual cortex, or attention-networks exert a higher influence on the behavioral maturation of scene perception than expected—at least in the tasks that we employed. Overall, our results suggest that behavioral proficiency in scene perception or memory and neural indices of scene processing capacity do not necessarily mature in unison.

4.5. Future directions

With the present study, we provide novel insights in the development of a category-selective network of high environmental importance. Yet, our study did not seek to answer the question whether environmental changes (such as learning the way to a new school) shape the neural scene-network development or whether it is this neural development that drives cognitive and behavioral changes such as better navigation. As stated in the interactive specialization framework (Johnson, 2011), these two factors might not be mutually exclusive but interdependent. Although manipulating children's experience with scenes over extended periods of time is challenging, we provide the basis for direct testing of the interactive specialization framework with scene stimuli.

Data and code availability statement

All code used for data analysis and stimulus presentation as well as anonymized raw data are publicly available at the Open Science Framework (https://osf.io/aydqz/, https://doi.org/10.17605/osf.io/aydqz).

Ethics statement

The Ruhr University Bochum Faculty of Psychology ethics board approved the study (proposal no. 280). All participants as well as children's parents gave informed written consent to participate voluntarily.

Conflicts of interest

The authors report no conflict of interest.

Acknowledgements

We thank our team of student assistants and interns for assisting in stimulus creation, pilot testing, subject recruiting, and data collection. We thank Kilian Semmelmann for input concerning the coding of the experimental paradigm and its implementation at the scanner. We thank Ruhr University Bochum's Biopsychology department for sharing resources. We acknowledge the support of the Neuorimaging Centre of the Research Department of Neuroscience at Ruhr University Bochum's teaching hospital and neurological clinic Bergmannsheil. Finally, we thank all participants and their parents for participating in this study.

This work was supported by a PhD scholarship of the Konrad-Adenauer-Foundation and an International Realization Budget of the Ruhr University Bochum Research School PLUS through funds of the German Research Foundation's Universities Excellence Initiative (GSC 98/3) to TWM, a PhD scholarship of the German Academic Scholarship Foundation to MN, and grants from the German Research Foundation (WE 5802/1-1), the Mercator Research Center Ruhr (AN-2014-0056), and the Volkswagen Foundation (Lichtenberg Professorship, 92 093) to SW.

Appendix A. Supplementary data

Supplementary data to this article can be found online at https://doi.org/10.1016/j.neuroimage.2019.02.025.

References

Afraz, S.-R., Kiani, R., Esteky, H., 2006. Microstimulation of inferotemporal cortex influences face categorization. Nature 442 (7103), 692–695. https://doi.org/10.1038/nature04982.

Baldassano, C., Esteva, A., Fei-Fei, L., Beck, D.M., 2016. Two distinct scene-processing networks connecting vision and memory. eNeuro 3 (5). https://doi.org/10.1523/ENEURO.0178-16.2016.

Bettencourt, K.C., Xu, Y., 2013. The role of transverse occipital sulcus in scene perception and its relationship to object individuation in inferior intraparietal sulcus. J. Cognit. Neurosci. 25 (10), 1711–1722. https://doi.org/10.1162/jocn_a_00422.

Bonner, M.F., Epstein, R.A., 2017. Coding of navigational affordances in the human visual system. Proc. Natl. Acad. Sci. U.S.A. 114 (18), 4793–4798. https://doi.org/10.1073/pnas.1618228114.

Brainard, D.H., 1997. The psychophysics toolbox. Spatial Vis. 10 (4), 433–436.

Brodeur, M.B., Dionne-Dostie, E., Montreuil, T., Lepage, M., 2010. The Bank of Standardized Stimuli (BOSS), a new set of 480 normative photos of objects to be used as visual stimuli in cognitive research. PLoS One 5 (5), e10773. https://doi.org/10.1371/journal.pone.0010773.

Brodeur, M.B., Guerard, K., Bouras, M., 2014. Bank of Standardized Stimuli (BOSS) phase II: 930 new normative photos. PLoS One 9 (9), e106953. https://doi.org/10.1371/journal.pone.0106953.

Burgund, E.D., Kang, H.C., Kelly, J.E., Buckner, R.L., Snyder, A.Z., Petersen, S.E., Schlaggar, B.L., 2002. The feasibility of a common stereotactic space for children and

adults in fMRI studies of development. Neuroimage 17 (1), 184–200. https://doi.org/10.1006/nimg.2002.1174.
Cantlon, J.F., Pinel, P., Dehaene, S., Pelphrey, K.A., 2011. Cortical representations of symbols, objects, and faces are pruned back during early childhood. Cerebr. Cortex 21 (1), 191–199. https://doi.org/10.1093/cercor/bhq078.
Chai, X.J., Ofen, N., Jacobs, L.F., Gabrieli, J.D.E., 2010. Scene complexity: influence on perception, memory, and development in the medial temporal lobe. Front. Hum. Neurosci. 4 (21), 21. https://doi.org/10.3389/fnhum.2010.00021.
Cukur, T., Huth, A.G., Nishimoto, S., Gallant, J.L., 2016. Functional subdomains within scene-selective cortex: parahippocampal place area, retrosplenial complex, and occipital place area. J. Neurosci. 36 (40), 10257–10273. https://doi.org/10.1523/JNEUROSCI.4033-14.2016.
Day, M.C., 1975. Developmental trends in visual scanning. In: Reese, Hayne (Ed.), Advances in Child Development and Behavior, first ed., vol. 10. Academic Press, Cambridge, MA, pp. 153–193.
Dehaene-Lambertz, G., Monzalvo, K., Dehaene, S., 2018. The emergence of the visual word form: longitudinal evolution of category-specific ventral visual areas during reading acquisition. PLoS Biol. 16 (3), e2004103. https://doi.org/10.1371/journal.pbio.2004103.
Dilks, D.D., Julian, J.B., Kubilius, J., Spelke, E.S., Kanwisher, N., 2011. Mirror-image sensitivity and invariance in object and scene processing pathways. J. Neurosci. 31 (31), 11305–11312. https://doi.org/10.1523/JNEUROSCI.1935-11.2011.
Dilks, D.D., Julian, J.B., Paunov, A.M., Kanwisher, N., 2013. The occipital place area is causally and selectively involved in scene perception. J. Neurosci. 33 (4), 1331. https://doi.org/10.1523/JNEUROSCI.4081-12.2013.
Dirks, J., Neisser, U., 1977. Memory for objects in real scenes: the development of recognition and recall. J. Exp. Child Psychol. 23 (2), 315–328. https://doi.org/10.1016/0022-0965(77)90108-4.
Epstein, R., Harris, A., Stanley, D., Kanwisher, N., 1999. The parahippocampal place area: recognition, navigation, or encoding? Neuron 23 (1), 115–125.
Epstein, R., Kanwisher, N., 1998. A cortical representation of the local visual environment. Nature 392 (6676), 598–601. https://doi.org/10.1038/33402.
Epstein, R.A., 2008. Parahippocampal and retrosplenial contributions to human spatial navigation. Trends Cognit. Sci. 12 (10), 388–396. https://doi.org/10.1016/j.tics.2008.07.004.
Epstein, R.A., Higgins, J.S., Thompson-Schill, S.L., 2005. Learning places from views: variation in scene processing as a function of experience and navigational ability. J. Cognit. Neurosci. 17 (1), 73–83. https://doi.org/10.1162/0898929052879987.
Epstein, R.A., Parker, W.E., Feiler, A.M., 2007. Where am I now? Distinct roles for parahippocampal and retrosplenial cortices in place recognition. J. Neurosci. 27 (23), 6141–6149. https://doi.org/10.1523/JNEUROSCI.0799-07.2007.
Ganaden, R.E., Mullin, C.R., Steeves, J.K.E., 2013. Transcranial magnetic stimulation to the transverse occipital sulcus affects scene but not object processing. J. Cognit. Neurosci. 25 (6), 961–968. https://doi.org/10.1162/jocn_a_00372.
Golarai, G., Ghahremani, D.G., Whitfield-Gabrieli, S., Reiss, A., Eberhardt, J.L., Gabrieli, J.D.E., Grill-Spector, K., 2007. Differential development of high-level visual cortex correlates with category-specific recognition memory. Nat. Neurosci. 10 (4), 512–522. https://doi.org/10.1038/nn1865.
Golarai, G., Liberman, A., Grill-Spector, K., 2017. Experience shapes the development of neural substrates of face processing in human ventral temporal cortex. Cerebr. Cortex 27 (2), 1229–1244. https://doi.org/10.1093/cercor/bhv314.
Golarai, G., Liberman, A., Yoon, J.M.D., Grill-Spector, K., 2010. Differential development of the ventral visual cortex extends through adolescence. Front. Hum. Neurosci. 3, 80. https://doi.org/10.3389/neuro.09.080.2009.
Gomez, J., Barnett, M.A., Natu, V., Mezer, A., Palomero-Gallagher, N., Weiner, K.S., Amunts, K., Zilles, K., Grill-Spector, K., 2017. Microstructural proliferation in human cortex is coupled with the development of face processing. Science 355 (6320), 68–71. https://doi.org/10.1126/science.aag0311.
Green, D.M., Swets, J.A., 1988. Signal Detection Theory and Psychophysics. Peninsula Publ, Los Altos, Calif., p. 505
Grill-Spector, K., 2003. The neural basis of object perception. Curr. Opin. Neurobiol. 13 (2), 159–166. https://doi.org/10.1016/S0959-4388(03)00040-0.
Grill-Spector, K., Golarai, G., Gabrieli, J., 2008. Developmental neuroimaging of the human ventral visual cortex. Trends Cognit. Sci. 12 (4), 152–162. https://doi.org/10.1016/j.tics.2008.01.009.
Grill-Spector, K., Sayres, R., Ress, D., 2007. High-resolution imaging reveals highly selective nonface clusters in the fusiform face area. Nat. Neurosci. 10 (1), 133. https://doi.org/10.1038/nn0107-133.
Harel, A., Kravitz, D.J., Baker, C.I., 2013. Deconstructing visual scenes in cortex: gradients of object and spatial layout information. Cerebr. Cortex 23 (4), 947–957. https://doi.org/10.1093/cercor/bhs091.
Hasson, U., Harel, M., Levy, I., Malach, R., 2003. Large-scale mirror-symmetry organization of human occipito-temporal object areas. Neuron 37 (6), 1027–1041. https://doi.org/10.1016/S0896-6273(03)00144-2.
Helle, C., Perona, P., 2000. Pasadena Houses 2000 Database. Computational Vision at California Institute of Technology. http://www.vision.caltech.edu/archive.html. (Accessed 11 January 2019).
Jiang, P., Tokariev, M., Aronen, E.T., Salonen, O., Ma, Y., Vuontela, V., Carlson, S., 2014. Responsiveness and functional connectivity of the scene-sensitive retrosplenial complex in 7-11-year-old children. Brain Cogn. 92C, 61–72. https://doi.org/10.1016/j.bandc.2014.10.005.
Johnson, M.H., 2011. Interactive specialization: a domain-general framework for human functional brain development? Dev Cogn Neurosci 1 (1), 7–21. https://doi.org/10.1016/j.dcn.2010.07.003.
Kamps, F.S., Julian, J.B., Kubilius, J., Kanwisher, N., Dilks, D.D., 2016. The occipital place area represents the local elements of scenes. Neuroimage 132, 417–424. https://doi.org/10.1016/j.neuroimage.2016.02.062.
Kang, H.C., Burgund, E.D., Lugar, H.M., Petersen, S.E., Schlaggar, B.L., 2003. Comparison of functional activation foci in children and adults using a common stereotactic space. Neuroimage 19 (1), 16–28. https://doi.org/10.1016/S1053-8119(03)00038-7.
Kanwisher, N., McDermott, J., Chun, M.M., 1997. The fusiform face area: a module in human extrastriate cortex specialized for face perception. J. Neurosci. 17 (11), 4302–4311. https://doi.org/10.1523/JNEUROSCI.17-11-04302.1997.
Kleiner, M., Brainard, D., Pelli, D., 2007. What's New in Psychtoolbox-3? Perception, vol. 36. ECVP Abstract Supplement). https://doi.org/10.1068/v070821 (0).
Mackworth, N.H., Bruner, J.S., 1970. How adults and children search and recognize pictures. Hum. Dev. 13 (3), 149–177. https://doi.org/10.1159/000270887.
Mandler, J.M., Robinson, C.A., 1978. Developmental changes in picture recognition. J. Exp. Child Psychol. 26 (1), 122–136. https://doi.org/10.1016/0022-0965(78)90114-5.
Mikellidou, K., Kurzawski, J.W., Frijia, F., Montanaro, D., Greco, V., Burr, D.C., Morrone, M.C., 2017. Area prostriata in the human brain. Curr. Biol. 27 (19), 3056–3060. https://doi.org/10.1016/j.cub.2017.08.065 e3.
Munsinger, H., Gummerman, K., 1967. Identification of form in patterns of visual noise. J. Exp. Psychol. 75 (1), 81–87. https://doi.org/10.1037/h0024890.
Nasr, S., Liu, N., Devaney, K.J., Yue, X., Rajimehr, R., Ungerleider, L.G., Tootell, R.B.H., 2011. Scene-selective cortical regions in human and nonhuman primates. J. Neurosci. 31 (39), 13771–13785. https://doi.org/10.1523/JNEUROSCI.2792-11.2011.
O'Craven, K.M., Kanwisher, N., 2000. Mental imagery of faces and places activates corresponding stiimulus-specific brain regions. J. Cognit. Neurosci. 12 (6), 1013–1023.
Park, S., Chun, M.M., 2009. Different roles of the parahippocampal place area (PPA) and retrosplenial cortex (RSC) in panoramic scene perception. Neuroimage 47 (4), 1747–1756. https://doi.org/10.1016/j.neuroimage.2009.04.058.
Pelli, D.G., 1997. The VideoToolbox software for visual psychophysics: transforming numbers into movies. Spatial Vis. 10 (4), 437–442.
Pelphrey, K.A., Lopez, J., Morris, J.P., 2009. Developmental continuity and change in responses to social and nonsocial categories in human extrastriate visual cortex. Front. Hum. Neurosci. 3, 25. https://doi.org/10.3389/neuro.09.025.2009.
R Core Team, 2015. R: A Language and Environment for Statistical Computing, Vienna, Austria. http://www.R-project.org/.
Scherf, K.S., Behrmann, M., Humphreys, K., Luna, B., 2007. Visual category-selectivity for faces, places and objects emerges along different developmental trajectories. Dev. Sci. 10 (4), F15–F30. https://doi.org/10.1111/j.1467-7687.2007.00595.x.
Scherf, K.S., Luna, B., Avidan, G., Behrmann, M., 2011. What" precedes "which": developmental neural tuning in face- and place-related cortex. Cerebr. Cortex 21 (9), 1963–1980. https://doi.org/10.1093/cercor/bhq269.
Simmons, W.K., Bellgowan, P.S.F., Martin, A., 2007. Measuring selectivity in fMRI data. Nat. Neurosci. 10 (1), 4–5. https://doi.org/10.1038/nn0107-4.
Talairach, J., Tournoux, P., 1988. Co-planar Stereotaxic Atlas of the Human Brain: 3-dimensional Proportional System : an Approach to Cerebral Imaging. Thieme, Stuttgart.
Thomason, M.E., Burrows, B.E., Gabrieli, J.D.E., Glover, G.H., 2005. Breath holding reveals differences in fMRI BOLD signal in children and adults. Neuroimage 25 (3), 824–837. https://doi.org/10.1016/j.neuroimage.2004.12.026.
Vurpillot, E., 1968. The development of scanning strategies and their relation to visual differentiation. J. Exp. Child Psychol. 6 (4), 632–650. https://doi.org/10.1016/0022-0965(68)90108-2.
Weigelt, S., Koldewyn, K., Dilks, D.D., Balas, B., McKone, E., Kanwisher, N., 2014. Domain-specific development of face memory but not face perception. Dev. Sci. 17 (1), 47–58. https://doi.org/10.1111/desc.12089.
Xiao, J., Ehinger, K.A., Hays, J., Torralba, A., Oliva, A., 2016. SUN database: exploring a large collection of scene categories. Int. J. Comput. Vis. 119 (1), 3–22. https://doi.org/10.1007/s11263-014-0748-y.
Xiao, J., Hays, J., Ehinger, K.A., Oliva, A., Torralba, A., 2010. SUN database: large-scale scene recognition from abbey to zoo. In: 2010 IEEE Conference on Computer Vision and Pattern Recognition(CVPR), pp. 3485–3492. https://doi.org/10.1109/CVPR.2010.5539970.
Zhen, Z., Kong, X.-Z., Huang, L., Yang, Z., Wang, X., Hao, X., Huang, T., Song, Y., Liu, J., 2017. Quantifying the variability of scene-selective regions: interindividual, interhemispheric, and sex differences. Hum. Brain Mapp. 38 (4), 2260–2275. https://doi.org/10.1002/hbm.23519.